Draft version September 1, 2011
Preprint typeset using LaTeX style emulateapj v. 11/10/09

OHMIC DISSIPATION IN HOT JUPITERS

Xu Huang[1] and Andrew Cumming[2]

Draft version September 1, 2011

ABSTRACT

We present an isolated analytical model for the ohmic heating in the interior of hot jupiters, treating the wind zone as a parameterized boundary condition. Under a conserved estimation of the strength of induced field and the assumption of an isothermal-convective planet model, we conclude that the mechanism of ohmic heating may not explain the over-inflated radius of hot jupiters along. We also develop a new time dependent evolution model for hot jupiters with ohmic heating, further show that ohmic heating is important only when the planet mass is small or the planet is at late stage of evolution.

1. INTRODUCTION

A puzzling property stands out ever since the discovery of the very first transiting planet HD209458b is the abnormally large radius of a significant large fraction of transiting planet. (Baraffe et al. 2010) Guillot & Showman (2002) pointed out that if certain amount of heating ($\sim 1\%$ stellar flux) can be deposited in the convection zone of the planet, then the over-inflated radius can be explained. But how to bring the required energy down to the interior of planet remains to be a question. Several explanations are proposed, such as a downward kinetic flux due to atmosphere circulation, and tidal dissipation. But each have problem to account for all observed radius.

Batygin & Stevenson (2010) provided a new magnetohydrodynamic mechanism to serve as the heating source in the interior of over-inflated hot jupiters. The idea is to transfer the kinetic energy of the flow in the wind zone into the ohmic power by generating an induced current from the dipole field of the planet. The downward part of the induced current will bring the energy inside the convection zone and dissipation the ohmic power in the interior. Perna et al. (2010a,b) also pointed out the possible importance of magnetic drag on the dynamics of the flow in the atmosphere, and also found a significant amount of energy could be dissipated by Ohmic heating.

Here we want to apply this idea to a new aspect of view, by separately considering the planet interior and wind zone. The aim is first to explore the parameter space and independently examine the physics in different layers of the atmosphere that influence the amount of ohmic heating. We also further introduce in a new evolution model, allowing ourselves to focus on the time history of planet entropy, and discuss various possibilities of planet evolution routines, expanding beyond Batygin et al. (2011)'s restriction on constant ohmic power.

The plan of the paper is as following: We will describe our toy models for interior ohmic heating in section §2. Then in §3 we are going to discuss the basic elements that build up the model. After that, we will present our results for both steady states models and time evolution models in §4.

[1] Department of Astrophysics Science, Princeton University, USA
[2] This work is a report for 2011 ISIMA project
[3] McGill University, Canada

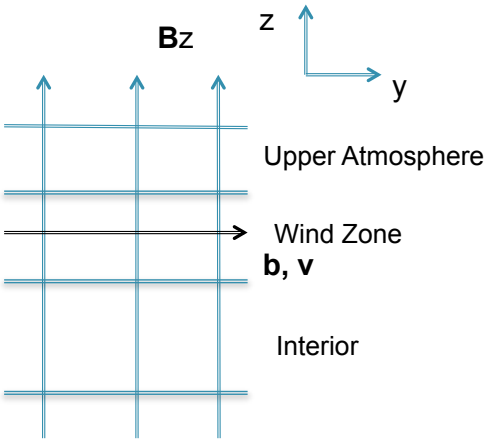

Fig. 1.— The plane parallel model configuration: A vertical field B_z is sheared by the wind v_y in the wind zone. An induced field b is produced by the shear.

2. DISTRIBUTION OF INDUCED CURRENT

2.1. *Plane Parallel Model*

To first look at the general property of the magnetic field and induced current, we develop a plane parallel model, divide the planet into three layers, representing the out most isothermal layer, with pressure lower than 30mbar, the wind zone, between 30mbar and 10bar and the interior of the planet, as in Figure 1, from top to bottom.

As shown in Figure 1, vertical field $\vec{B}$ is sheared by the wind in the wind zone. The shearing velocity is described by $v_y(z)\exp(ikx)$. An induced field $\vec{b}$ is generated by solve the induction equation Eq 1.

$$\frac{\partial \vec{B}}{\partial t} = -\nabla \times \eta(\nabla \times \vec{B}) + \nabla \times (\vec{v}/c \times \vec{B}) \qquad (1)$$

in which, η is the resistivity profile, $\eta = \frac{c^2}{4\pi\sigma}$. This induced field can penetrates the interior of the planet and provide a vertical current inside. Because there is no wind in the interior, the induced equation is simplified as $\nabla \times (\eta \nabla \times \vec{b}) = 0$. If we assume the conductivity is constant, the solution gives $\vec{b} = e^{\pm kz}\hat{y}$ and $j_z = ikb$. Both the field and current decrease exponentially in the interior, leaves a surface layer in the interior with thickness $2\pi/k$. A more general case of this model can be

presented as Eq 2.

$$\frac{d^2b}{dz^2} - k^2 b + \frac{d\eta}{dz}\frac{db}{dz} = 0 \tag{2}$$

The solution is similar, however, the variation of conductivity σ on the depth z can change the thickness of the surface layer.

2.2. *Spherical Shell Model*

Based on the analysis for the plane parallel model, we can figure out that the properties of the field and current in the interior of planet is only determined by three factors: the geometry of the shearing velocity in the wind zone, the magnitude of the induced field at the top of the convection zone and the profile of the conductivity in the interior. And the both of the first two factors can be turn into boundary conditions if we want to focus on the interior only. Since the heating inside convection zone is the most important part for inflating the planet and the wind zone is complicate for simple consideration, we will separately considerate these two layers. In this part, we will first estimate what boundary condition we can generate from the wind zone and then process detailed calculation in the interior layer. The position of the layers are the same as in the plane parallel model, and the radiative/convective boundary is taken at approximately 100bar. In this way, we can have a good understanding of the importance of ohmic heating for hot jupiters.

We consider a simple geometry with a dipole field and an one jet wind sheared in the $\hat{\theta}$ direction $\vec{v} = v_0 \sin\theta\,\hat{\phi}$. The induced toroidal field produced by this shearing geometry is $\vec{B_\phi} = B_{\phi 0}\sin\theta\cos\theta\hat{\phi}$. We seek for a steady states for the induction equation Eq 1 in spherical coordinates. In the interior, where $\vec{v}\times\vec{B} = 0$, the equation reduced to be

$$\nabla \times \eta(\nabla \times B_\phi\hat{\phi}) = 0 \tag{3}$$

Assume spherical symmetric, we can decompose the induced field into a radial component and an angle component. $B_\phi(r) = \frac{g(r)}{r}Y_{20}$. By eliminate the angle component, we obtain

$$g''(r) - \frac{d\ln\sigma}{dr}g'(r) - l(l+1)\frac{g(r)}{r^2} = 0 \tag{4}$$

$l = 2$ is the index of spherical homonic Y_{20}. This can be analytical solved when σ has a power-law dependence on radius. When $\sigma \propto r^\alpha$, the solution is

$$g(r) \sim r^{\frac{(1+\alpha)+\sqrt{(1+\alpha)^2+24}}{2}} \tag{5}$$

With the Ampere's law $\vec{J} = \frac{c}{4\pi}\nabla\times\vec{B}$, we obtain a radial component of current J_r in the interior, and the angle component J_θ vanishes at the boundary of the wind zone. The power in the interior can be calculated as

$$P = \int\int \frac{J_r^2}{\sigma} r^2 \sin\theta\, d\theta\, d\phi \tag{6}$$

A specific case is when conductivity is constant. $\alpha = 0$, so that the solution of $g(r)$ reduce to $\propto r^3$. And the induced field and radial current are simply $B_\phi \propto r^2$ and $J_r \propto r$.

3. INGRIDIANT OF THE MODEL

In this section, we are going to discuss several ingredients in the calculation. The first component is the influence of the geometry in the wind zone. The second is the strength of induced field in the boundary of wind zone. The third is to the profile of conductivity in the interior.

3.1. *Geometry of the Shearing Velocity*

Though the geometry of the velocity profile in the wind zone is complicated and uncertain, we can have some simple prescriptions by assuming azimuthal symmetry. The shearing velocity can be written with $v_\phi \propto \sin l\theta$ to represent a retrograde motion, as a more general expression for examples in Batygin et al. (2011), which gives a spherical hormonic with the lth order Y_{l0}. A solution with constant conductivity from Eq 5 gives $B \propto r^l$. It indicates, the more zonal jets in the profile of wind zone, the shallower the induced field penetrates inside the planet.

3.2. *Magnitude of the Induced Field*

From the balance between the diffusion of the dipole field and the generation of the induced field, we can obtain:

$$\frac{B_\phi}{B_r} = R_M = \frac{4\pi\sigma H v_\phi}{c^2} \tag{7}$$

in which, H is the local pressure scale height and v_ϕ is the averaged wind speed. When the wind speed is taken to be 1km/s, the strength of induced field is

$$B_\phi = B_r \frac{\sigma}{10^{-3}\mathrm{S/m}}\frac{H}{0.01R_J}\frac{v_\phi}{1\mathrm{km/s}} \tag{8}$$

There are two major consideration to constrain the strength of the likely upper atmosphere field B_r. Sánchez-Lavega (2004) argued that the field is generated by the dynamo action in the metallic region, as in Jupiter (Stevenson 1983). Field strength is closely related to the rotation of the planet, with $B \sim (\rho\Omega\lambda_B)^{\frac{1}{2}}$, this predicts that the field on typical hot jupiters should be a factor of few smaller than that on the Jupiter, the typical value of equator field is approximately $B_{eq} \sim 5$G. However, an opposite point of view gives a more optimistic estimation. Christensen et al. (2009) argue that the field is more dependent on the heat flux escaping from the conductivity core when the rotation rates exits an upper limit. $B \sim (\rho F_{core}^2)^{\frac{1}{3}}$. In this way, the strength of field on hot jupiter might be a order of magnitude larger than estimated with the previous method.

3.3. *profile of conductivity in the interior of hot jupiters*

The conductivity in the upper atmosphere of hot jupiters is dominate by the ionization of alkali metal, for the surface temperature is not high enough to ionize hydrogen and helium; on the contrast, in the hot interior core with high pressure, the ionization hydrogen dominates the conductivity.

There are a set of alkali metal which can contribute to the conductivity in the atmosphere. We first look at potassium which has the lowest ionization potential. From the Saha equation,

$$x = \left[\frac{f_k}{n}\left(\frac{m_e k_B T}{2\pi\hbar^2}\right)^{3/2} e^{-4.35\mathrm{eV}/k_B T}\right]^{\frac{1}{2}}$$

$$= 1.03 \times 10^{-3} T_3^{5/4} e^{-25.19/T_3} (\frac{f_K}{10^{-7}})^{1/2} (\frac{P}{1\text{bar}})^{-1/2} \quad (9)$$

We then put in Na, Fe, Mg with the same method, but it turns out they are not as important as the role of potassium as long as the temperature is lower than 2000K. The conductivity is then determined by the collision of electron and neutron hydrogen. $\sigma = \frac{n_e e^2}{m_e \nu} = 3.1 \times 10^{15} x / T_4^{1/2}$, with the collision frequency $\nu = n_n \langle \sigma v \rangle_e$ given by Draine et al. (1983) as:

$$\langle \sigma v \rangle_e = 10^{-15} (\frac{128kT}{4\pi m_e})^{1/2} \text{cm}^3\text{s}^{-1} \quad (10)$$

In the deeper part of the planet, the hydrogen is ionized by high pressure and the conductivity is dominated by electron-proton collision. In the fully degenerated limit, $\nu_{epd} = 4e^4 m_e \Lambda / 3\pi\hbar^2 = 1.8 \times 10^{16}\text{s}^{-1}$. In the non-degenerated limit, $\nu_{epnd} = 5 \times 10^{14}\text{s}^{-1}(1 - Y_e)$. We interpolate between this two limits to give an estimation of the total contribution.

The comparison of the two parts of contribution to the electron fraction and the conductivity are shown in Figure 2(a).

Under more careful consideration, there exists a transition phase which will dominate the conductivity when the temperature is high enough so that the conductivity due to the alkali metals are small and the pressure is not high enough to ionize the hydrogen. Liu et al. (2006) pointed out, before the fully ionization of hydrogen molecule, the band-gap of hydrogen will diminish with the increase of pressure. This insulator to conductor transition can be written as a semiconductor conductivity:

$$\sigma = \sigma_0 exp(\frac{-E_g(\rho)}{k_B T}) \quad (11)$$

Between 0.2Mbar and 1.8Mbar, $E_g = 20.3 - 64.7\rho$, where E_g is in eV, and ρ is in mol. $\sigma_0 = 3.4 \times 10^{20} exp(-44\rho)\text{s}^{-1}$. While between 0.1Mbar and 0.2Mbar, $\sigma_0 = 0.5 \times 10^{18}\text{s}^{-1}$. Figure 2(c) is the final conductivity profile for the planet. Noted that though conductivity σ varies with pressure in almost ten magnitudes, when look at the radius space, it's nearly constant in the interior of the planet.

4. RESULT AND DISCUSSION

4.1. *Analytical Result*

We can estimate the power from the ohmic heating per unit mass by taken $P_m = J^2/(\sigma\rho)$. Here we assume $\sigma = const$ is a good approximation, then we can take $B_\phi(r) \propto r^2$ and $J_r \propto r$. If we fixed the field strength at the bottom of the wind zone, then

$$P_m = \frac{J^2}{\sigma\rho} = \frac{B_{\phi 0}^2}{r^2 \sigma \rho} (\frac{c}{4\pi})^2 \quad (12)$$

$$= 10^{-1} \text{erg/s/g} (\frac{B_\phi}{10\text{G}})^2 (\frac{r}{R_J})^{-2} (\frac{\sigma}{10^6\text{s}^{-1}})^{-1} (\frac{\rho}{10^{-4}\text{g/cm}^3})^{-1}$$

$$= 10^{-15} \text{erg/s/g} (\frac{B_\phi}{10\text{G}})^2 (\frac{r_c}{10^{-4} R_J})^{-2} (\frac{\sigma}{10^{16}\text{s}^{-1}})^{-1} (\frac{\rho}{1\text{g/cm}^3})^{-1}$$

Eq 12 displays the possible heating per unit mass at the top of the convection zone and the very center of the planet. We can indicate from this that the heating is dominated by the top layer of the convection zone. The overall heating deposited in the interior then can be estimated as:

$$P_{ohm} = 4\pi P_{top} R^2 \rho H = 10^{16}\text{W} (\frac{B_{\phi 0}}{10\text{G}})^2 (\frac{\sigma_t}{10^6\text{s}^{-1}})^{-1} (\frac{H}{0.01 R_J}) \quad (13)$$

In which, σ_t is the conductivity at the top of the convection zone, and H is the scale height of effective heating layer. This total amount of heating is not strongly dependent on the radial current profile in terms of pressure. Since we scale with the top most induced current, only the heating in the highest pressure region will be sensitive to the radius dependence of induced current, but it is negligible when compare to the overall heating. Therefore, it's also a good approximation if taking the interior current as a constant.

4.2. *Fixed Structure Model*

The magnetic field structure in the planet interior is obtained by solving Eq 3 for a preset conductivity profile in Figure 2(c). This conductivity profile is calculated for a planet structure built up from the inside out by

$$\frac{dM}{dr} = 4\pi\rho r^2 \quad (14)$$

$$\frac{dP}{dr} = -\rho \frac{GM}{r^2} \quad (15)$$

$$\frac{dT}{dr} = \frac{T}{P} \nabla \frac{dP}{dr} \quad (16)$$

For this paticular model, we make the center temperature and pressure to be $T_c = 3 \times 10^4$K, $P_c = 2 \times 10^7$bar. We also take the isothermal sphere temperature $T_{iso} =$ 1400K and the induced magnetic field $B_\phi = 10$G at $P =$ 100bar as the out boundary condition. (Here after we call this model our standard model.)

We set $\nabla = \nabla_{ad}$ when $T > T_{iso}$ so the planet is adiabatic in the interior; after the temperature decreases to T_{iso} from inside out, we make the planet isothermal. The EOS is taken with helium fraction $Y = 0.25$. The solved planet structure is shown in Figure 3. The solution for induced field, the ohmic power per unit mass and the integrated ohmic power are shown in Figure 4. We integrate the power below $P = 100$bar, which gives $P_{ohm}(P \geqslant 100\text{bar}) = 9.68 \times 10^{15}$W. We over-plotted the final solutions with analytical result from Eq 12 when assuming $B \propto r^2$ (red and dashed line in Figure 4(b), 4(c)) . The comparison indicates it is quite a good approximation if we only want to estimate the ohmic power with an order of magnitude accuracy. Batygin & Stevenson (2010) reported in their HD209458b model an ohmic power of 1.09×10^{16}W for the same set of parameters. However, we also calculate a model with helium fraction $Y = 0.3$, which gives $P_{ohm}(P \geqslant 100\text{bar}) = 9.70 \times 10^{15}$W. This indicates that the ohmic power we obtain in the interior of planet is hardly related with the helium fraction, depart from what's shown in the Table 1 of Batygin & Stevenson (2010).

Since we want to further look into the feed back of ohmic heating to the structure of planet, we modify our

equation set above, add in heating term as:

$$\nabla = \min(\nabla_{rad}, \nabla_{ad}) \tag{17}$$

$$\nabla_{rad} = \frac{3\kappa L}{16\pi cGM}\frac{P}{aT^4} \tag{18}$$

$$\frac{dL}{dr} = 4\pi r^2\rho(\epsilon - T\frac{ds}{dT}) = \int \frac{J^2}{\sigma}\, dV - 4\pi r^2 \rho T \frac{ds}{dT} \tag{19}$$

$$J = \frac{c}{4\pi}\nabla\times B_\phi \tag{20}$$

$$\nabla\times(\eta\nabla\times B_\phi) = 0 \tag{21}$$

Here we are required to consider the opacity carefully inside the planet. We compute our opacity by combine the interpolated data from Freedman's radiative opacity table and Potekhin's conductivity opacity table. The Rosseland mean opacity is obtained by $\kappa = (\kappa_{rad}^{-1} + \kappa_{cond}^{-1})^{-1}$. In the intermediate pressure range where neither opacity tables cover, we assume the scaling $\kappa \propto P^{0.5}$. Opacity profile for our standard model is shown in Figure 5, over-plotted with opacity taken from MESA using the same planet structure. We can see there is some disagreement, especially between $10^3 - 10^5$bar.

If we consider the steady state solution only, then $\frac{dL}{dr} = 4\pi r^2\rho\epsilon$. Since the ohmic power is small in the center of the planet and the opacity drops in high pressure region due conductivity opacity, it might be difficult to keep the planet convective by heating only.

We estimated how much heating is needed to make the inner core convective by setting $\nabla_{ad} = \nabla_{rad}$. Form Eq 22, we can see this requirement far exceeds what we are able to get from the ohmic heating. If we want to keep the model convective, cooling flux is required. Since the cooling flux varies from time, it's necessary to make a time dependent model.

$$\frac{J^2}{\sigma\rho} = \frac{16\pi acT^4 G\nabla_{ad}}{3\kappa P} \tag{22}$$

$$= 10^{-6}\mathrm{erg/s/g}(\frac{T_c}{3\times10^4\mathrm{K}})^4(\frac{\kappa}{3\mathrm{cm^2/g}})^{-1}(\frac{P_c}{2\times10^7\mathrm{bar}})^{-1}(\frac{\nabla_{ad}}{0.3})$$

4.3. *Time Dependent Result*

Inspired by the approach of Arras & Bildsten (2006), we compute our time dependent model in a statistic survey way, instead of doing time integration for a particular model. The assumptions are as following: a) all the models we are looking for are fully convective inside and isothermal outside, which means the sum of the cooling flux and ohmic heating is large enough to keep the interior convective. b) the $B_\phi \propto r^2$ law is a good approximation for all the models when calculates the amount of ohmic power dissipated in the interior. c) the induced field $B_{\phi 0}$ at the bottom of the wind zone is kept to be constant due to some mechanism, one of the most likely reason is the magnetic Reynolds number is limited to order of 1 by magnetic drag on the wind. d) All the planet with the same mass follows the same entropy time history.

Based on these assumptions, we build a number of models by varying center entropy S_c and pressure P_c in a large parameter space. ($6 < S_c < 10$, $10^2\mathrm{bar} < P_c < 10^9\mathrm{bar}$). From these models, we are able to calculate the corresponding cooling flux for a different models. If no heating is involved, the cooling flux equals to the luminosity of the planet. The planet luminosity L is defined as the radiative luminosity calculated at the isothermal/convective boundary, with $\nabla_{rad} = \nabla_{ad}$.

$$-M\bar{T}dS/dt = L = \frac{16\pi GcM_r}{3\kappa P}aT^4\nabla_{ad} \tag{23}$$

We use $\bar{T}$ to represent the mass weighted average temperature, and M_r is the mass inside the convection zone. If we bin the models into different masses, we can reproduce the evolution history for a fixed planet mass by integrating forward in time for the entropy. In Figure 6, we compare our result with Paxton et al. (2011) for the cooling history of Jupiter mass planet. (Note: here I need to over-plot with Paxton's data). It's interesting that we find out the ratio between planet luminosity and mass is a function only depend on the center entropy of the planet, as seen in the green lines of Figure 7.

When ohmic heating is under consideration, the cooling flux and the ohmic heating power provide the planet luminosity together:

$$dS/dt = -(L - \int J^2/\sigma\, dV)/(\bar{T}M)$$

We compute the time history of the planet luminosity and ohmic power in the same way as the cooling only case in Figure 8. We can see that as the planet is cooling, the ohmic power of the planet is increasing, and gradually dominates the contribution of the cooling flux. After the ohmic power dominates the cooling flux, our assumption of fully convective planet may not be valid any more. Fortunately, the thermal timescale inside the planet already becomes really long after this critical age, and the planet entropy is maintained by the ohmic heating deposited in the planet interior. So we can view the evolution afterwards as a quasi steady state. We notice that planets with smaller mass can obtain a higher ohmic power, and reach steady states earlier. We also plot the relation between interior ohmic power and center entropy for different mass planets in the red lines of Figure 7. The fitting indicates that the interior ohmic power is likely inverse proportion to the planet mass.

It's important to ask what's the age of a planet with a particular mass when reaches a steady state. In Figure 9, we report that the result is sensitive to the strength of $B_{\phi 0}$. For $B_{\phi 0}$ equals 10G, a $0.3M_J$ hot jupiter can reach steady states in 1Gyrs, while a $1M_J$ hot jupiter will take longer than 100Gyrs to cool. (Here we set the isothermal sphere temperature to be 1400K.)

We can also vary the isothermal sphere temperature and estimated the required $B_{\phi 0}$ to make the planet enter steady states within 1Gyrs. We find that, in Figure 10, for hotter planet, stronger induced field is needed to obtain important ohmic heating. This is because the interior ohmic heating is closely related to the conductivity at the bottom of the wind zone; while the conductivity increase with temperature, the ohmic heating reduce if induced field is fixed. But we should also point out, for hotter planet, there is higher chance to obtain stronger induced field due to stronger wind in the atmosphere. So this result does not simply mean it is more difficult to make ohmic heating important in hotter planet.

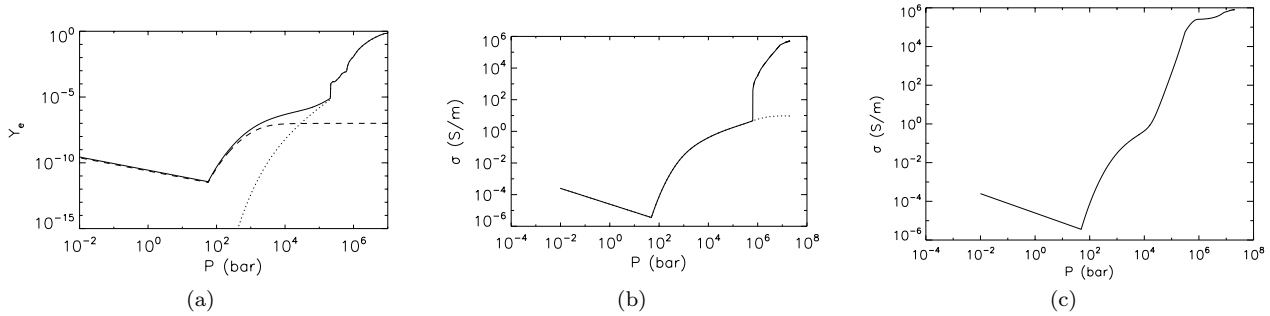

(a) (b) (c)

FIG. 2.— From left to right: a) the electron fraction contribution of different component. Dashed: potassium; Dotted: ionized hydrogen; Solid: potassium and ionized hydrogen. b) the conductivity contribution of different component. Dotted: potassium; Solid: total contribution with potassium and ionized hydrogen. c) the final profile of conductivity with all three components.

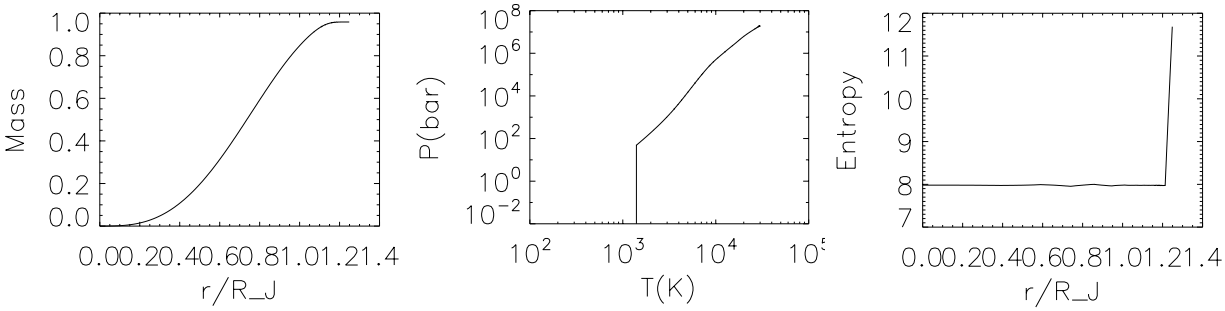

FIG. 3.— structure profile. From left to right: mass radius relationship of model, final planet mass is $0.96M_J$, radius is $1.25R_J$; thermal structure of model, planet atmosphere turn to be isothermal above $P = 100$bar; entropy profile of planet, center entropy is ~ 8, outer entropy is ~ 12.

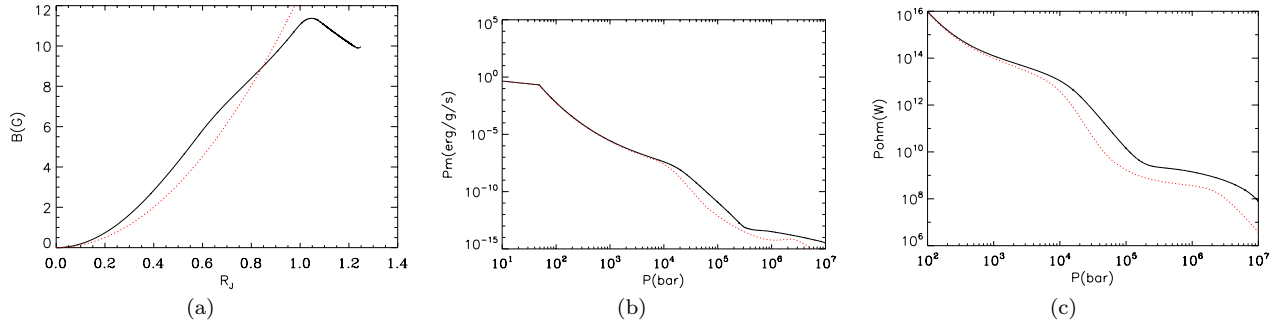

(a) (b) (c)

FIG. 4.— From left to right: a) the solution of magnetic field versus radius (Black and solid line) over-plotted with fitting function $B \propto r^2$ (Red and dashed line). b) The power per unit mass versus pressure (Black and solid line) over-plotted with result from assuming $B \propto r^2$ (Red and dashed line). c) The integrated power versus pressure (Black and Solid line) over-plotted with result from assuming $B \propto r^2$.

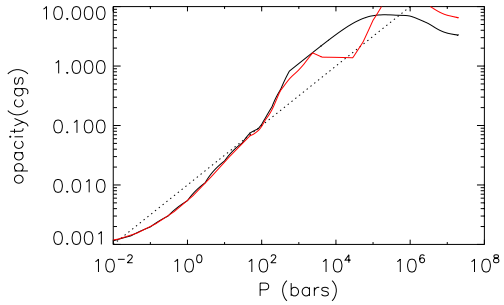

FIG. 5.— The opacity profile of the model by combine two tables as mentioned in the text. (Solid). MESA opacity (Red Solid). Opacity approximated by $\kappa \propto P^{0.5}$. (Dotted)

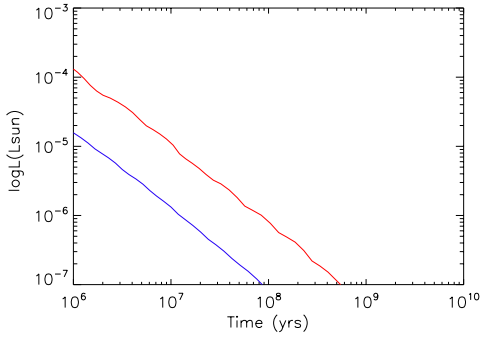

FIG. 6.— The cooling curve without heating for $1M_J$ (Blue) and $3M_J$ (Red) planet calculated from our time dependent model. Note: Here we need to over-plot these with referenced data.

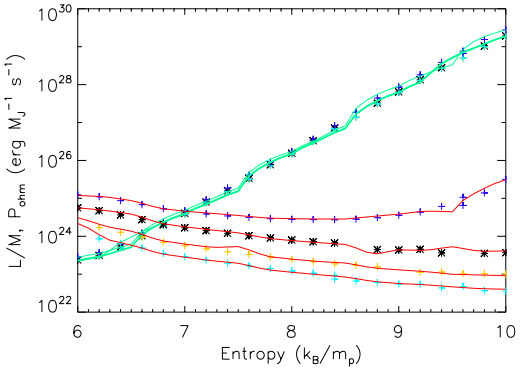

FIG. 7.— Mass weighted planet luminosity and the interior ohmic heating versus center entropy. Blue cross, black asterisk, yellow cross, light blue cross represent planets in different mass bins: $0.3M_J$, $1.0M_J$, $3.0M_J$, $6.0M_J$. Green lines are the fitting for L/M versus S, mass is in the units of M_J. Red lines are the fitting for P_{ohm} versus S. L/M is only the function of S, $L = Mf(S)$. For fixed enter entropy, the planet with smaller mass can obtain a higher ohmic power.

If we look at the final radius resulted from ohmic heating with $B_\phi = 10G$ and assuming $T_{iso} = 1400K$ for different planet mass, they are obvious not inflated enough to explain the observed radius. (Figure 11) For example, HD209458b has a observed radius of $1.35R_J$ with mass $0.7M_J$, while we can only obtain a radius of $1.25R_J$ from the calculation. This is because the power we introduced into the planet interior is far smaller than the received stellar luminosity. In the case of our standard model,

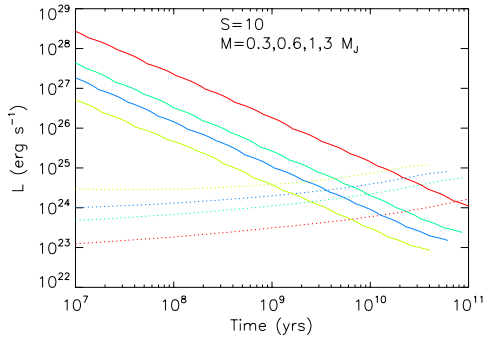

FIG. 8.— The time history of planet luminosity and ohmic heating for $0.3M_J$ (Yellow), $0.6M_J$ (Blue), $1M_J$ (Green) and $3M_J$ (Red) planet. Planet luminosity decrease with time because of cooling, while the ohmic heating increase with time. The crossing point of the two lines indicates where the ohmic heating provides all the planet luminosity.

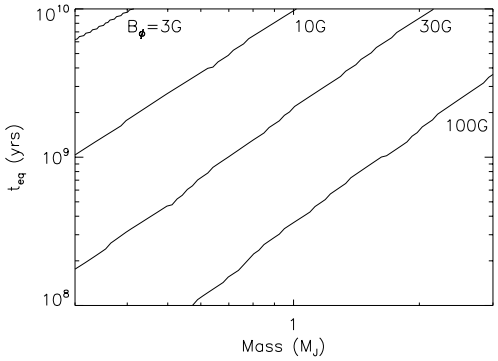

FIG. 9.— The age of planet when ohmic heating dominates versus planet mass, different lines are calculated with models assuming B_ϕ at the bottom of the wind zone to be 3G, 10G, 30G, 100G.

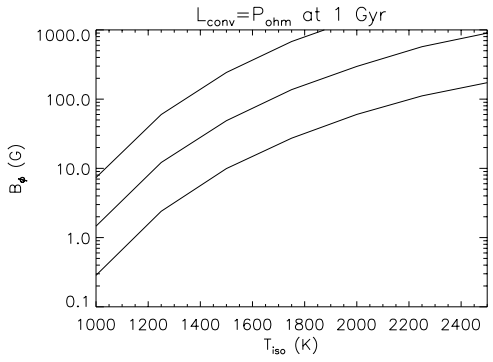

FIG. 10.— The strength of magnetic field required for ohmic heating to dominate inside 1Gyrs versus the isothermal sphere temperature. Different lines are calculated with models with different planet mass: $0.3M_J$, $1M_J$ and $3M_J$.

the stellar luminosity is 10^{22}W, and the heating in the interior is only one millionth of it, 10^{16}W. However, in this prediction, we limit our model with conserved input parameter so that the ohmic heating looks incapable to explain the observed radius alone. There are several uncertainties that might make the situation more optimistic, we will discuss each of them separately in the following section.

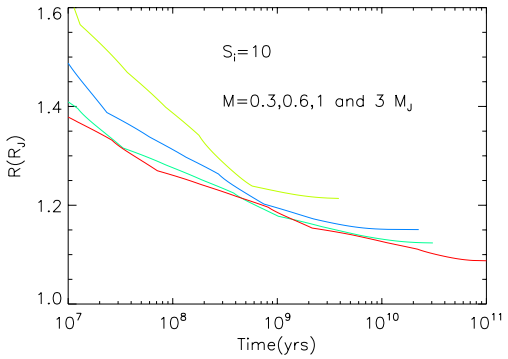

FIG. 11.— The time history of planet radius with different planet mass. Red: $3M_J$, Green: $1M_J$, Blue: $0.6M_J$ and Yellow: $0.3M_J$. All the models are calculated with $B_\phi = 10$G.

4.4. *Limitation of the model*

As described above, under all the assumptions we make, if ohmic heating itself can provide an explanation to the over-inflated radius of hot jupiters is questionable. However, there are several significant uncertainties due to the boundary conditions from the wind zone.

First, the strength of the induced field B_ϕ generated by the wind is not well constrained. We've already discussed the uncertainties risen from the dipole field B_r in §3.2. A factor more difficult to be determined is the limit of the magnetic Reynolds number R_M. Recall that this dimensionless number depends on the product of conductivity and wind speed. While the conductivity increase with temperature exponentially, will the strength of induced field also increase unlimited? We already know a R_M large enough will bring in additional physics such as dynamo. And there are several other possibilities that might limit the amplitude of B_ϕ. Among them, magnetic drag and turbulence diffusivity are two major issues. (This part should be discussed more detailed later on). But an exact upper limit of the field is not set. At this stage, we consider R_M equals an order of unity to be a reasonable approximation by inserting typical numbers of conductivity and wind speed from hot jupiter's atmosphere. By doing this, we limit ourselves under a maximum amount of heating and neglecting the possibility of thermal instability result from the sharp dependence of conductivity on temperature. Also, in our treatment, the induced field is an independent parameter from the planet properties such as T_{iso} and central entropy, which might not be true in real case. In general, a hotter isothermal atmosphere is able to produce stronger induced field, for the planet receive more energy from the stellar flux.

Second, the position of wind zone as well as the radiative/ convective boundary is not well defined. We've been ignoring the existence of a radiative layer between the isothermal atmophere and the convection zone and chose $P = 100$bar as our isothermal/convective boundary. At the same time, we fix the wind zone at $P = 10$bar. These choices are reasonable for our standard model. However, the position of the radiative/convective boundary varies a lot with different central entropy. Studies show that a $S = 8$ planet may have a much deeper convection zone than a $S = 10$ planet. Since the total interior heating is dominate by the surface layer of the convection zone, significant change will present when we move this boundary. Meanwhile, in the early stage of evolution, when the radiative/convective boundary is at low pressure (lower than $P = 10$bar, we need to re-justify the validity of the assumption that the position of wind zone is at 10bar.

5. CONCLUSION

In this project we present a toy model which carefully reconstruct the ohmic heating in the interior of hot jupiters. With boundary condition chosen to represent the typical properties of wind zone, we can obtain the level of heating deposited in the convection zone and examine its significance to the evolution of the planet. We also introduce in a new way to look into the time dependent evolution model, though which, we reproduce the time history of hot jupiter under different conditions of ohmic heating. If limit our model to a reasonable estimation of the isothermal temperature $T_{iso} = 1400$K and a induced field $B_\phi = 10G$, we find out that ohmic heating won't be important for the evolution of a $1M_J$ planet before 10Gyrs and the radius of planet already shrinks to a value that small than what's observed. We can imply from this conclusion that either additional heating method is needed to explain to enormous radius or we need to relax our restrictions of the model to increase the amount of heating inject inside the convection zone.

To be conclude, future effort need to be made in realistic models for the atmosphere circulation so that better constrain can be obtain for the interior heating. Models with radiative zone are also worth to be checked more carefully for it determines where the boundary of interior sits.

We thank the organizers of the 2011 ISIMA program, held in Kavli Institute of Astronomy & Astrophysics in Beijing. We would like to thank Yanqin Wu and Yoram Lithwick for useful discussion.

REFERENCES

Arras, P., & Bildsten, L. 2006, ApJ, 650, 394
Baraffe, I., Chabrier, G., & Barman, T. 2010, Reports on Progress in Physics, 73, 016901
Batygin, K., & Stevenson, D. J. 2010, ApJ, 714, L238
Batygin, K., Stevenson, D. J., & Bodenheimer, P. H. 2011, arXiv:1101.3800
Christensen, U. R., Holzwarth, V., & Reiners, A. 2009, Nature, 457, 167
Draine, B. T., Roberge, W. G., & Dalgarno, A. 1983, ApJ, 264, 485
Guillot, T., & Showman, A. P. 2002, A&A, 385, 156
Liu, J., Goldreich, P. M., & Stevenson, D. J. 2006, Bulletin of the American Astronomical Society, 38, 483
Paxton, B., Bildsten, L., Dotter, A., Herwig, F., Lesaffre, P., & Timmes, F. 2011, ApJS, 192, 3
Perna, R., Menou, K., & Rauscher, E. 2010, ApJ, 719, 1421
Perna, R., Menou, K., & Rauscher, E. 2010, ApJ, 724, 313
Sánchez-Lavega, A. 2004, ApJ, 609, L87
Stevenson, D. J. 1983, Reports on Progress in Physics, 46, 555
Trammell, G. B., Arras, P., & Li, Z.-Y. 2011, ApJ, 728, 152